Composites: Part A 167 (2023) 107425

Contents lists available at ScienceDirect

Composites Part A

journal homepage: www.elsevier.com/locate/compositesa

Exploring the role of fibre sizing to the fatigue of glass fibre composites using a novel, reliable micro-fatigue test

P. Laurikainen [a,*], R. Dsouza [a], M. Kakkonen [b], M. Kanerva [a], E. Sarlin [a]

[a] Tampere University, Faculty of Engineering and Natural Sciences, PO Box 589, FI-33014 Tampere University, Finland
[b] Fibrobotics Oy, Finland

ARTICLE INFO

Keywords:
Interface/interphase
Interfacial strength
Fatigue
Microbond test

ABSTRACT

Single fibre micro-composite tests are among the most reliable methods for characterising the fibre–matrix interphase. To improve their versatility, this study utilises a well-characterised microbond setup in a cyclic loading case to create a so-called micro-fatigue test. The surface of the fibres is controlled to create two distinctive interphase types: a clean glass fibre surface, and a model sizing. The sizing improved the average interfacial performance in all tested cases, but the role of the sizing was most prominent in the fatigue lifetime of the microdroplet samples. Finite element analysis was used to evaluate the strain-rate dependency and heating related to the plastic deformation of the microdroplet samples in cyclic loading and predicted a well behaving experimental setup. The method offers a promising pathway for further studies on interfacial fatigue and the role of sizing in it.

1. Introduction

Fibre-reinforced composites find a variety of applications in the automotive and aerospace industries due to their high strength-to-weight ratio. However, to get the most out of the composite material the fibre–matrix interface cannot be ignored, as the stress transfer from the matrix to the fibres is crucial in order to reach the full potential of the material. In glass fibre composites, this stress transfer is ensured with the use of specific surface treatments on the fibre surface, the most common by far being a thin coating known as sizing. Commercial sizing comprises both components for improving interfacial performance – such as coupling agent and film former – and processing aids that improve wetting, protect the fibre and otherwise ease the handling during further process steps [1]. When the fibres are coated with resin, the sizing mixes partially with the resin, creating the interphase: a region distinctive from both fibre and matrix and of significant importance to the overall composite performance. Thus, experimental approaches for measuring the properties of this interphase region have seen considerable research effort in the past decades and resulted in fairly well established quasi-static micro-composite experiments, such as the pull out and microbond tests [2]. These tests are frequently used to determine the local interfacial parameters such as shear strength and fracture toughness of the interface.

Many – if not most – composite products are utilised in applications that result in fatigue due to vibrations, varying wind loads or even impacts, and the performance of the interphase in such applications is almost impossible to predict from quasi static experiments. Unstable crack propagation is difficult to measure using these quasi-static destructive tests and detailed analysis of dissipative and non-dissipative energy contributions is not possible. These factors are only observable through cyclic loading tests and could provide valuable information on the nature of the interphase in terms of, for example, viscoelasticity. A successful microcomposite fatigue test would also enable the much needed opportunity to study the fatigue failure process at the interphase without the influences of fibre breaks and fibre-fibre interactions, which contribute significantly in macroscale fatigue [3].

Currently, only a few examples for this type of test are found in literature. Combining the complexity of microcomposite testing to the already complex case of cyclic loading presents a significant challenge. As with quasi-static microcomposite testing, the underlying phenomena and the limitations of the device must be addressed to ensure the measured property has any physical meaning to actual composite performance.

Mai et al. [4] have tested cyclic loading in microscale based on the pull out scheme. The test uses a piezoelectronics-based transducer to achieve cyclic loading with position and force recording. The tests themselves comprise frequency sweeps to determine the phase angle and loss factor (tan δ). In a sense, the test in this case could be compared to a microcomposite dynamic mechanical analysis (DMA). Mäder et al. [5] and Brodowsky et al. [6] have later used the same setup to

* Corresponding author.
E-mail address: pekka.laurikainen@tuni.fi (P. Laurikainen).

https://doi.org/10.1016/j.compositesa.2023.107425
Received 29 October 2022; Received in revised form 16 December 2022; Accepted 2 January 2023
Available online 4 January 2023

perform a type of fatigue testing with altering strain amplitude and frequency and reported significant improvement in fatigue lifetime for high stress loading when their model sizing was used to improve the apparent interfacial adhesion. They also noted that the improvement was far lesser for low stress dynamic loading [5]. The embedded length ranges for the tests in question were between 100–800 μm with the displacement amplitudes varying up to two microns [6]. No explicit description on number of tested samples is given, but the presented data focuses on single measurements per sample type.

Shin et al. [7] have used a microbond-based cyclic loading scheme to explore the effects of dopamine as a compatibiliser – or coupling agent – between glass fibres and epoxy. The test utilised relatively high levels of pre-stress followed by cyclic loading of the pre-stressed state. The results showed minor improvement in fatigue behaviour under cyclic loading with the addition of dopamine. However, the testing setup was based on a universal testing system and both the number of tested samples and the number of cycles in the test were very low.

Several theories exist on how the sizing applied on fibre surface helps create the improved interfacial contact observable in actual macroscale composites — ranging from covalent bonding of the coupling agent to both fibre and matrix, to simply plasticising and toughening of the matrix by the low molecular weight sizing components. Both of these likely contribute to the properties of real interphases with relative contributions changing based on the used sizing [8,9]. The interphase could be described as a gradient shift in composition from covalently and hydrogen bonded coupling agent [1,8], film former and matrix. Such a structure would hypothetically offer both the improved interfacial contact – via an interpenetrating network of matrix and the sizing connected to the fibre surface, not excluding the possibility of direct covalent bonding – and an altering of matrix properties in relation to bulk matrix. Cyclic loading of microcomposites of the appropriate scale range could provide valuable insights into the performance of this region and thus help understand also the interphase structure in more detail.

So, many questions about the nature of the interphase and its performance under cyclic loading still remain. In the context of microcomposite testing, however, among the greatest issues is still the discussion around scale related issues in resin properties and whether microcomposite tests in general have any correlation with macroscale [10–12]. Further work is needed to bridge the gap in qualitative understanding of the correlation between structure and composition the properties of the interphase, determining how quantitative the results can be, and how to utilise the results in composite design. Incorporating finite element analysis (FEA) has proven an increasingly effective tool for predicting test related phenomena, which remain otherwise difficult to observe [13]. Incorporating FEA in the analysis can therefore both help understand the phenomena and validate the experimental approach.

Here, we present an efficient micro-fatigue test based on the microbond concept for characterising composite interphases. Reliability was achieved by the collection of a large range of data to analyse the fatigue properties of the interface, and thorough characterisation of the testing setup to minimise device and test related contributions. On average 10 to 15 droplets were measured per single filament and the effect of fibre sizing was analysed based on both fatigue life performance and an in-depth analysis of the micromechanics, using FEA, based on the recorded force-strain data. Each test was performed as cyclic tensile loading (R ratio = 0) test with near-constant peak force until the droplet was completely sheared from the fibre. The damage propagation at the interface during cyclic loading was analysed and the contributions of dissipative and non-dissipative energies were evaluated. The heating of the micro-droplet due to the plastic deformation, the strain strain-rate dependency of the results and the role of friction in the test were explored through FEA.

2. Materials and methods

2.1. Experimental

The experimental setup for fatigue testing was based on the FIBRObond device [14]. The only major modification was the change of the displacement actuator from a DC motor to a magnetic linear actuator capable of rapid accelerations and near frictionless operation — both crucial for this type of cyclic testing. During the test, the drive was operated at a speed of 2.0 mm/s, with the displacement amplitude varying based on the droplet embedded length and the desired load level for each test. The resulting frequency range was 6–10 Hz depending on the displacement amplitude of each measurement. The higher strain-rate – compared to the quasi-static microbond test – was expected to affect results but the increased rate was also necessary to control the time required for a single measurement. The role of strain-rate was evaluated in Section 2.2.

Early on, an issue was identified where the peak force level gradually decreases as the test progresses, both due to the plastic deformation of the droplet at the beginning of the measurement and possibly the propagation of the damage in the later stages. To keep the peak strain (and force) as constant as possible throughout the measurement, an algorithm was added to the measurement control that monitors the peak force levels and compensates for any changes over time with approximately 0.5–3.5 micrometer shifts to the starting position of the cyclic displacement along the fibre axis. The exact value for each compensation was dependent on the displacement amplitude and the stage of the measurement. Preliminary tests supported the initial hypothesis that the later stage compensation events correspond to propagating damage in the microcomposite sample, and thus, were logged into the measurement outputs as a potential qualitative measure of damage evolution. To better understand the loading state in terms of strain – an inarguably important part of any fatigue consideration – the fiber Bragg grating (FBG) sensor solution presented by Dsouza et al. [13] was used to monitor the fibre strain to provide additional input for FEA.

For fibres, an old batch of Jushi ECR-17 glass fibre roving, was treated with pirahna solution to remove any organic sizing or residues from the fibre surface. Half of the cleaned fibres were then resized with a 1% non-volatile content solution comprising 3-aminopropyl triethoxysilane (10%) and Hydrosize EP871EU epoxy dispersion (90%), kindly supplied by Michelman (Michelman International SARL, Luxembourg). The solution was used to create a fresh – and compositionally known – model sizing on the fibres. These two fibre types are denoted as unsized and sized fibres, respectively, in this study.

Several dozen droplets of Araldite 5052 LY/Aradur 5052 (resin/hardener, 100/38 parts by weight) epoxy system were deposited on each single fibre, spanning a length of 14–15 mm between the points of support provided by the sample holder (see Fig. 1). The droplets were cured at 80 °C for eight hours. The droplets were debonded either with both quasi-static loading (microbond test) or cyclic loading (micro-fatigue test). The microbond test was to provide a direct point of comparison for the fatigue test results. For the microbond tests, the speed of the magnetic actuator was set to 0.008 mm/s.

2.2. Finite element analysis

A 3D finite element model (FE) of the test was developed using Abaqus Standard/Explicit 2020 (Dassault Systèmes, France). The droplet ($\phi_{droplet}$ = 0.036 mm and A_{embedded} = 0.102 mm) was chosen from the test of sized filament (ϕ_{fibre} = 0.0178 mm) located 6 mm from the fixed position of the fibre. A systematic approach was followed wherein the FE model was developed for a quasi-static microbond test using an implicit solver for static analysis (*FE1-static*) and the coupled temperature–displacement analysis (*FE2-accum* and *FE3-dissip*). To investigate the dynamic effects, the FE models were further simulated with an explicit solver (*FE4-dyn*). In all cases, the filament (fibre in test),

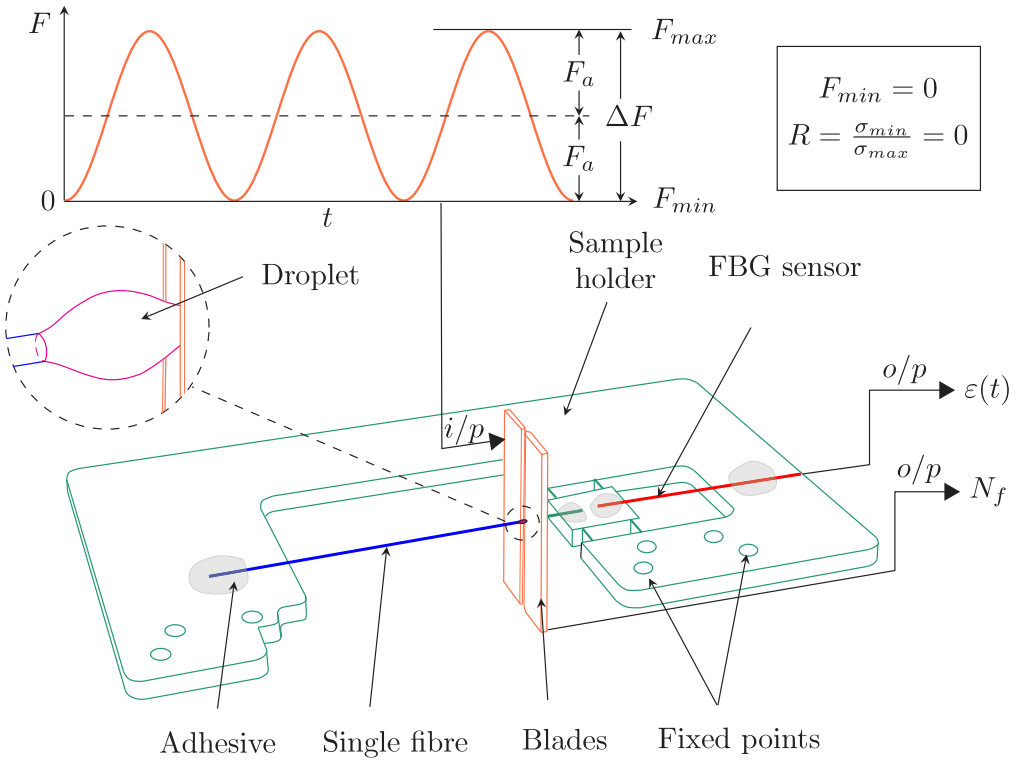

Fig. 1. Experimental arrangement of the microbond-based fatigue test used in the study. Here F_a, R, $\epsilon(t)$ and N_f represent force amplitude, fatigue stress ratio, time dependent strain and number of cycles to failure, respectively.

FBG sensor, sample holder and adhesive were modelled as linear elastic materials and the loading blades as rigid bodies (setup of FE model in Fig. 2). For the interface, surface-based cohesive zone modelling (CZM) was used with the maximum stress criterion for damage onset and a mixed-mode power law for damage evolution. Force and fibre strain data from the experiments were used to validate the interfacial constants such as critical stress (τ_c) and critical energy of debonding (G_c) using force-strain derivative data [15]. The interfacial constants were determined as τ_c = 50 MPa and G_c = 50 J/m^2 for the sized filament (used for all FE models in this paper). For the unsized filaments these constants are τ_c = 39 MPa and G_c = 44 J/m^2. It was assumed that the mode I component of G_c and τ_c behaved in the same way as the mode II and mode III components. In all cases, the epoxy droplet was treated as elastic–plastic with isotropic hardening conditions. The evolution of the plastic strain at different strain rates was incorporated into the *FE4-dyn* model (the data is provided in Supplementary Data S1). Details of the boundary conditions and numerical values of the mechanical constants can be found in previous publications [13,15]. The shrinkage of the droplet due to cooling from the curing temperature of 80 °C to a room temperature was simulated by including a temperature difference of −56 °C as a loading step in the analysis. For element types, linear brick elements with reduced integration (C3D8R) were used for *FE1-static* and *FE4-dyn*, whereas tri-linear displacement and temperature brick elements with reduced integration (C3D8RT) were used for *FE2-accum* and *FE3-dissip*.

The thermal material constants of the components at room temperature, which were used for the *FE2-coup* and *FE3-dissip* cases are provided in Table 1. The full, temperature dependent thermal conductivities and specific heats are provided in supplementary data S2 and S3, respectively. The convective heat transfer coefficient of 13 Wm^{-2} K^{-1} was defined as a film coefficient and was applied on the outer surface of the droplet and the fibre. A thermal conductance of 21 Wm^{-2} K^{-1} was used between the fibre and the droplet: the detailed explanation for this is provided in supplementary data S4. Only the inelastic deformation (90%) of the droplet was considered for the heat generation and no frictional component was modelled in the current simulations. It is also important to note that the heat originated due to the interfacial degradation is not taken into account for any of the FE simulations. The FE model attributes were set to a temperature of 24 °C for all the cases.

To study the effect of blade velocity during the cyclic test, a single cycle test was simulated at different displacement rates using *FE4-expl*. A displacement amplitude lower than the damage onset value was chosen and kept constant while the cycle time is varied to achieve certain displacement rate. A stable time increment was selected and kept constant ($\delta t = 8 \times 10^{-10}$ s). To simulate the cyclic testing, a cyclic load with constant peak force at different levels was provided as an input to the models and corresponding compensation of blade displacement was recorded. For friction, two different origins are considered relevant in this study. Friction at not fully debonded regions (adhesional friction) and at debonded regions (sliding friction), the former being very complex to observe or measure. Even for the sliding friction, a definitive value of the friction coefficient (μ) cannot be accurately determined from the values of the sliding force in the experiment (i.e. when the droplet slides on the fibre after debonding, denoted F_{fric}). A very thin residual film is formed at the droplet exit point during droplet preparation, which increases the experimental F_{fric}. This in turn leads to overestimated the values of μ and poses a challenge in estimating it. Thus, for the purpose of this study, friction is addressed qualitatively using FEA through μ values, which lie within reasonable limits for the tests. An isotropic Coulomb friction model is used in conjunction with the CZM. The temperature effects are investigated by simulating *FE3-dissip* with μ = 0.1, 0.3 and 0.5, where the fraction of friction converted to heat is defined as 100%. To explore the role of friction in the results, *FE4-expl* is simulated with μ = 0.1 and the number of input cycles is increased until the droplet debonds from the interface.

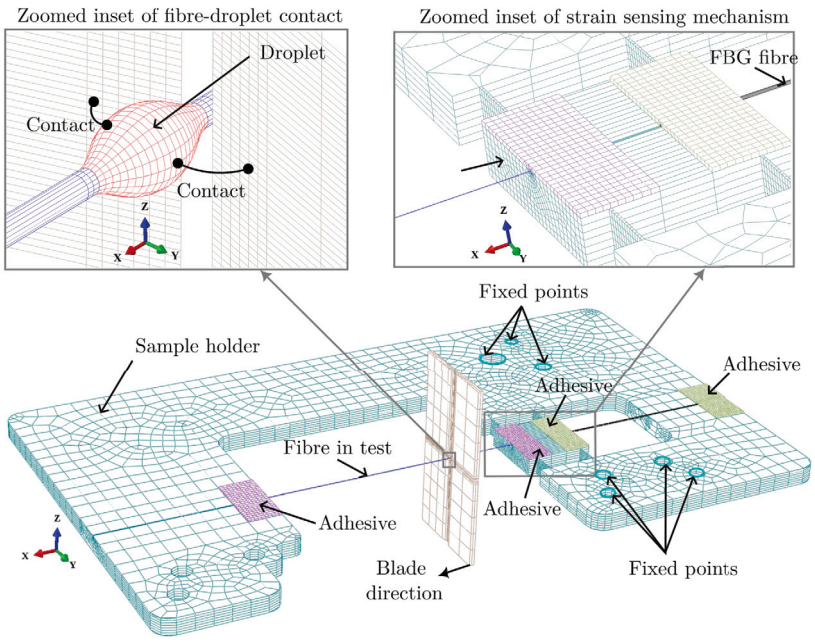

Fig. 2. Full setup of the FE model along with the zoomed insets.

Table 1
Values of the thermal material constants used in FE modelling.

Constituent	Thermal conductivity, K (W m^{-1} °C^{-1})	Specific heat (J kg^{-1} °C^{-1})	Coefficient of thermal expansion (×10^{-6}1 °C^{-1})	Source
Droplet	0.241[a]	237[a]	71[a]	in-house
Filament	1.3	805	4.1	[16,17]
Optical fibre	1.3	805	4.1	[16,17]
Sample holder	7.1	553	8.7	[18]
Blades	45	460	10.8	[19]
Adhesive	0.14	300	25	[b]

[a]Temperature dependent data available in the supplementary file.
[b]Generic adhesive values from different sources.

3. Results and discussion

3.1. Experimental results

A total of 117 droplets were measured with cyclic loading. Out of these, 108 were considered successful measurements. The rest comprised either fibre breakages or prematurely halted measurements — due to either run outs (i.e. tests run for 10^7 cycles without failure) or software problems. The scattering of the results was fairly high, which is expected in a fatigue test [20]. To ensure the comparability of the two data sets the embedded length ranges of the droplets were kept similar, i.e. 98.1 ± 12.9 μm for the unsized and 94.1 ± 11.2 μm for the sized fibres. The fibres were also similar in diameter: unsized fibres 18.3 ± 0.9 μm, sized fibres 18.3 ± 1.3 μm.

As the primary output of the fatigue testing, the stress-number of cycles (SN) curves for the two sample systems are presented in Fig. 3(a) and (b) along with results from the quasi-static (microbond) testing for comparison.

Fig. 3(c and d) show the Weibull probability plots for the cyclic tests separated into three apparent peak stress groups. The groups were selected by selecting the datapoints with average apparent stress levels during the test in the range of mean ±1/2× standard deviation of the whole dataset, with the high and low outliers forming the two other groups. The sized fibres outperformed the unsized fibres at all loading levels. The Weibull analysis indicates that at practically any comparable loading levels, the sized fibres have a smaller probability of failure. Therefore, it seems the sizing and the resulting interphase are crucial for the fatigue life under cyclic loads similarly to what was previously reported by Mäder et al. [5]. The Weibull fits were used to predict fatigue life (Nf) at probability levels 2.3% ($Nf_{2.3\%}$), 50 % ($Nf_{50\%}$) and 97.7% ($Nf_{97.7\%}$). For the average apparent stress levels of the two fibre types, these values are estimated as: $Nf_{2.3\%}$ of 5.8 (sized) and 3.2 (unsized), $Nf_{50\%}$ of 4780 (sized) and 2180 (unsized), and $Nf_{97.7\%}$ of 136 000 (sized) and 57 000 (unsized). The amount of data is, however, not sufficient for a more detailed analysis, and the results cannot be considered more than qualitative.

Analysis of the Pearson's linear correlation coefficients of the experimental outputs (peak force, fibre/droplet volume fraction) versus number of tested cycles reveals a significant difference between the two sample types. Volume fraction was selected as it combines all geometrical aspects of the drop-on-fibre sample and to avoid significant changes in sample behaviour – due to, for example, local stress fields, strain rate dependency or changes in resin degree of cure – the intent was to have a suitably narrow range of droplet sizes to minimise any correlation. Thus the result would mainly be dependent on the applied load. Analysis of variance (ANOVA) was utilised to identify deviating datasets based on the individual filaments, which could highlight problems in experimentation or sample preparation. The results of this analysis are presented in Fig. 4. The correlation analysis in Fig. 4 appears to distinguish two very different behaviours for the sample types where for sized fibres the tested number of fatigue cycles correlates most with the volume fraction i.e. the relative size of the droplet with little of the expected correlation with the applied peak force level while the reverse is true for the unsized fibres. The ANOVA,

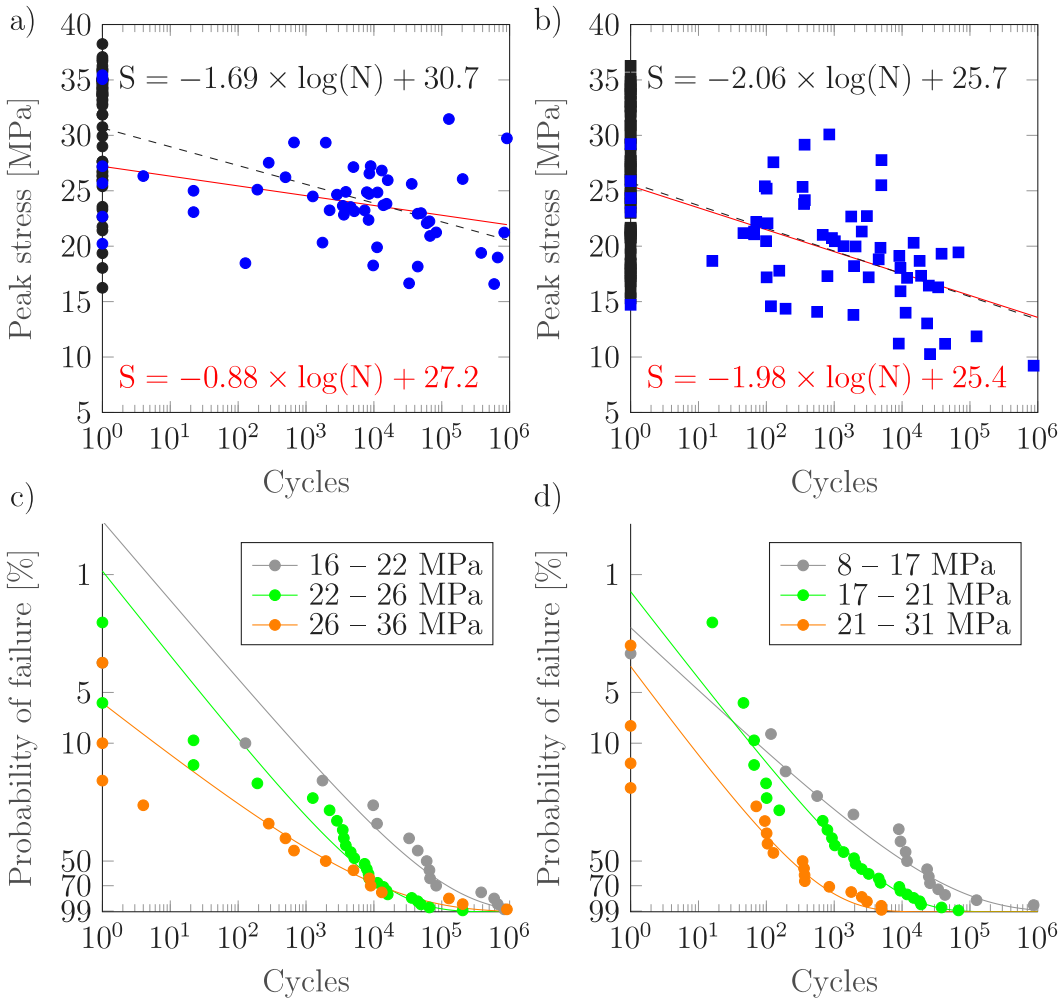

Fig. 3. Results of the fatigue testing, SN plot of (a) sized and (b) unsized fibres at R = 0 (displacement rate: 2.0 mm/s). Quasi-static results (displacement rate: 0.008 mm/s) presented for comparison in black. Red fitted curve: micro-fatigue results only. Dashed fitted curve: all results included. Weibull probability plots for sized (c) and unsized (d) fibres. Data is separated into three stress level groups signified in the legend.

however, revealed both complete datasets comprise several behaviour groups. For both sized and unsized fibres, the largest filament datasets follow the originally assumed behaviour: correlation mainly between peak force and number of cycles. Some correlation with droplet size is also noted for several datasets, while for some the number of measured droplets was too small to draw any reliable conclusions. Overall, this follows the behaviour reported earlier for the quasi-static test [14]: a significant portion of the scatter in the data arises from the variation between the individual filaments of the fibre bundle. The problem of high scatter of the results and the resulting poor correlation could be mitigated with either significantly more data, or by more extensive use of local parameters, such as the local strain recording [15], which in this study was mainly utilised for the purpose of FEA.

The sample deformation during the fatigue testing was observed by the compensations done by the algorithm to keep the load level constant. Examples are presented in Fig. 5 with arrows indicating the same compensation events in the peak force and number of compensation plots. The compensation counts in Fig. 5 hint at two very different damage evolution processes. The initial compensations – coinciding with the increasing load level – correspond to the plastic deformation of the meniscus at the blade contact and initial damage formation quite early in the measurement. In Fig. 5 these are observable as the frequent early compensations at steady intervals. This behaviour was also predicted by the FE simulation of multiple loading cycles (see Section 2.2). The progression of the deformation tended to differ between the two sample types. For the sized fibres, the rate of compensations was lower, possibly indicating the interphase is more stable. However, after a significant number of cycles, the rapid compensations indicated a quite rapid propagation of damage until failure. For the samples with no sizing, the rate of compensations remained consistent throughout the measurement. The behaviour correlates with the observations made during the measurements: the washed samples exhibited a generally more brittle behaviour.

Comparing the results with quasi-static method, i.e. the microbond test, revealed a similar difference in performance of the two fibre batches. The microbond results were measured from the same filaments as the fatigue testing to minimise the effect of variation between filaments, which has previously been shown to be quite significant [14]. The results of the microbond tests are presented in Fig. 6 as maximum force during the experiment vs. droplet embedded area ($A_{embedded}$) calculated from the droplet embedded length and fibre diameter.

The results are sufficient for comparative analysis. The amount of tested droplets was, however, slightly limited due to the increased risk of fibre breakage during and after the fatigue testing. The fibre breakages were caused either by a poor guess of the initial displacement amplitude causing a too high force level, or unexpected fibre failure due to the repeated loading cycles. The most common filament breaks were, however, caused during microbond testing of a fibre subjected to significantly over 10^7 loading cycles, i.e. after several droplets were measured in with cyclic loading. The stress levels on the filament during the cyclic

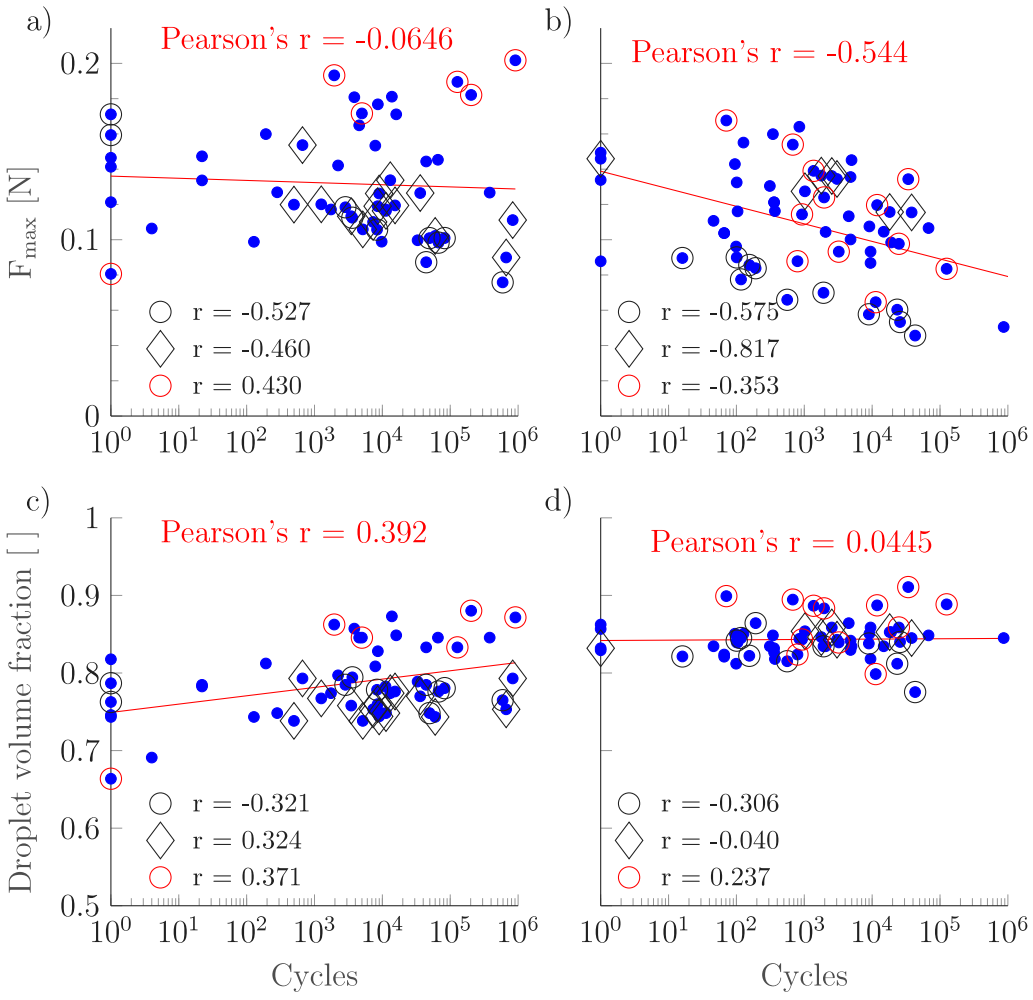

Fig. 4. Correlation analysis of different factors vs. the number of cycles. (a)–(b) Peak force (F_{max}) for sized and unsized fibres, respectively. (c)–(d) Droplet volume fraction for sized and unsized fibres, respectively. Overall Pearson's r for all data in red. Highlighted datapoints correspond to data from different individual filaments along with their Pearson's r values.

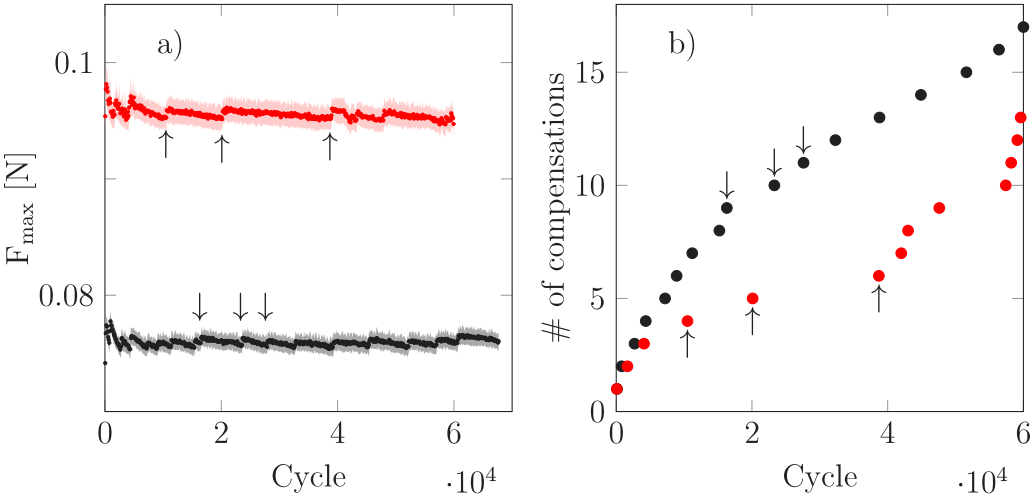

Fig. 5. Local averages and standard deviations (100 points) of load peaks (a) and compensations (b) for selected measurements of unsized (black) and sized (red) samples lasting approx. 67 000 and 60 000 cycles, respectively. The arrows indicate examples of corresponding compensation events in the two plots.

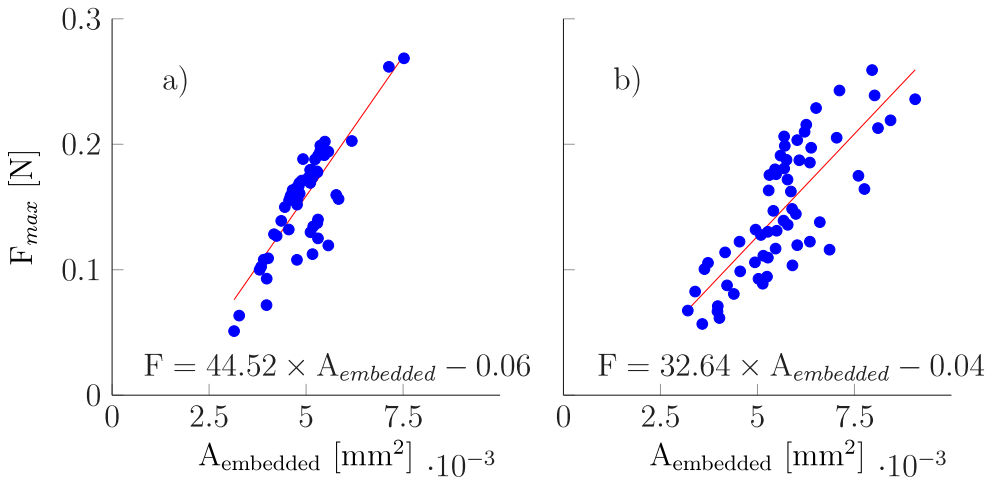

Fig. 6. Results of the quasi-static (microbond) tests for (a) sized (b) unsized fibres. $A_{embedded}$ is droplet embedded area.

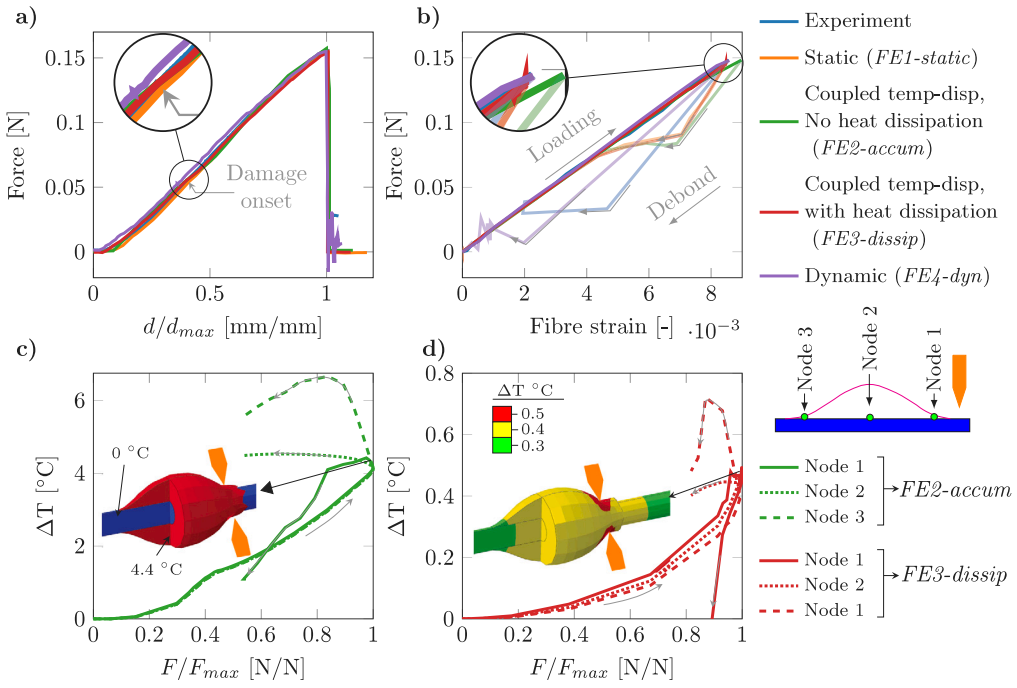

Fig. 7. Plot (a) force as a function of displacement; (b) output force as a function of fibre strain; (c,d) temperature at three different nodal points (close to the interface) from FE model as a function of force. Blade displacement (d) and force (F) are normalised with the corresponding d and F at the maximum value of force (F_{max}).

loading are low compared to the fibre ultimate properties and assumed to not affect the fibres excluding the aforementioned scenarios of fibre breakage.

3.2. FEA results

The FE simulation results for the quasi-static microbond test with different solvers are presented in Fig. 7(a)–(b). Except for *FE2-accum*, all the FE simulation results are in excellent agreement with the experimental force-fibre strain data, in-turn validating the interfacial constants used for the simulations. *FE2-accum*, deviates slightly from the experimental results as the accumulated heat in the droplet affects the interfacial damage.

Fig. 7(c)–(d) shows the distribution of temperature at three nodal points close to the interface. In the quasi-static case, a significant amount of heat was generated due to the plastic deformation of the droplet with $\Delta T \approx 7$ °C (Fig. 7(c)). This heat was dissipated to the fibre via thermal conduction and further to the surroundings through the fibre and the droplet surfaces. There was no physical heat transfer through convection in the FE model, but the effective heat transfer was simulated using the surface film coefficient, which mimics the effects of convection. Under these conditions, *FE3-dissip* simulation showed that ΔT does not exceed 0.7 °C for a quasi-static test. Therefore, the deformation related heating of the sample does not affect sample behaviour in the static tests.

FE simulations also enable the evaluation of the role of strain-rate in the test. The resin itself has clear strain-rate dependency (of modulus of elasticity) and similar effects are expected in the microdroplet scale. A single cycle test at the blade displacement rate of 0.1 mm/s is shown in Fig. 8(a)–(c), wherein the input single cycle is provided to the blades in the form of smooth amplitude displacement (b_d). The maxima of the different quantities (denoted with subindex "*max*") are plotted as a function of displacement rates as shown in Fig. 8(d)–(f). The maximum of the kinetic energy (KE_{max}) is way lower than the maximum of the

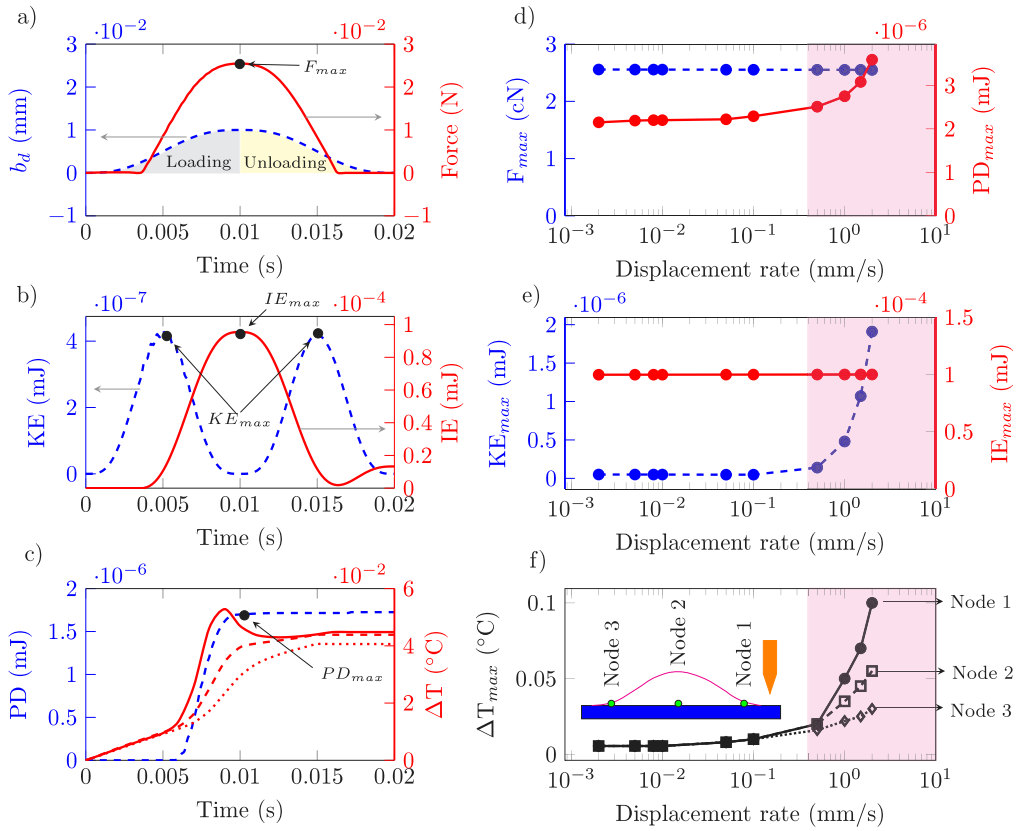

Fig. 8. (a)–(c) Results of FE simulations for a single cycle test at displacement rate 0.1 mm/s; (d)–(f) Results of FE simulations as a function of displacement rate.

internal energy (IE_{max}) up to a displacement rate of 0.5 mm/s. The micro-fatigue test exhibited dynamic behaviour when the displacement rate of the blades exceed 0.5 mm/s. This result is based on KE_{max} where a significant change in slope was observed. Similar behaviour was observed with the energy dissipated due to plastic deformation of the droplet (*PD*), which increases with the increase in displacement rate. This also led to the increase in the nodal temperatures (T_{max}). It is evident that the T_{max} was higher at Node 1, due to the higher rate of droplet deformation when compared to Node 2 and Node 3. As the micro-fatigue experiments were carried out at 2 mm/s, the tests were well within the strain rate range of these simulated dynamic effects.

For load levels corresponding to 25%, 60% and 80% of F_{max} (per simulated test), 20 consecutive input cycles were simulated and the results are presented in Fig. 9. The need for a steady increase in b_d was observed to keep the peak force per cycle constant. It is similar to the behaviour observed during the experiments, where a compensation is needed to keep the peak force level constant but actualised through a change of the zero position of b_d closer to the droplet. With an input force of 80% of F_{max} (0.12 N), the interface was completely debonded at 17 cycles. The crack initiates in the first cycle for all the cases. Comparing all the three force inputs (levels) one can observe a clear pattern in the growth of *PD* and energy dissipated due to interfacial damage and crack (*DMD*), with a non-linear rise of the curve at the start and abrupt rise at the end. For the initial blade contact with the droplet, contact area was lower at the meniscus, which promotes larger energy dissipation. This leads to the sudden rise of *PD* followed by a non-linear rise until the blades deform the meniscus region. The test becomes stable for a large number of cycles depending on the input force level, which represents the largest part of the cycles measured during the real test. For the case of complete debonding of the droplet, the undamaged area of the interface becomes so small, that the compensation of b_d increased drastically, which initiated an abrupt increase in *PD* and an unsteady propagation of *DMD*. At lower force levels, *PD* and *DMD* does not increase significantly during the first few cycles followed by a slow growth during the subsequent cycles. This increased the expected fatigue lifetime of the interface during cycling loading compared to cases where significant plastic deformation and interfacial damage were generated early.

3.3. Effect of interfacial friction

When studying friction effects, it is important to note that damage evolution is a mixed mode, allowing damage propagation in all three modes. The friction created between the fibre and the droplet in the damaged zone can lead to a temperature increase at the interface and in the fibre-droplet assembly. Comparing the temperature profiles of the quasi-static simulations (Fig. 10(a)), it is clear that the friction at the interface can drive up the heat release. The change in ΔT is not significant until the onset of damage because friction is not activated, whereas ΔT increases when friction at the interface is increased (3 °C maximum in ΔT). Subsequently, these changes are very significant after the droplet is debonded, as the increase in ΔT is only due to the frictional contact between the surfaces. Overall ΔT values are quite minimal and heating of the sample can be ruled out in the static tests.

In micro-fatigue testing, the friction between the fibre and the droplet at the damaged zone can significantly increase the fatigue tolerance. When damage initiates at the interface, the frictional force in the damaged region stabilises the damage propagation, resulting in an increased number of cycles, indicating a good fatigue tolerance. As an example, for the same input force profiles (Fig. 9(b)), the frictionless interface debonds in 17 cycles (Fig. 9(f)), while the interface with $\mu = 0.1$ debonds in 66 cycles (Fig. 10(b) and (c)). Larger friction between the fibre and the droplet leads to an increase in the number of cycles to failure. Furthermore, the damage propagation is steady and no exponential growth of *DMD* is observed as in the case of a frictionless interface. This is due to the energy dissipated due to friction (*FD*)

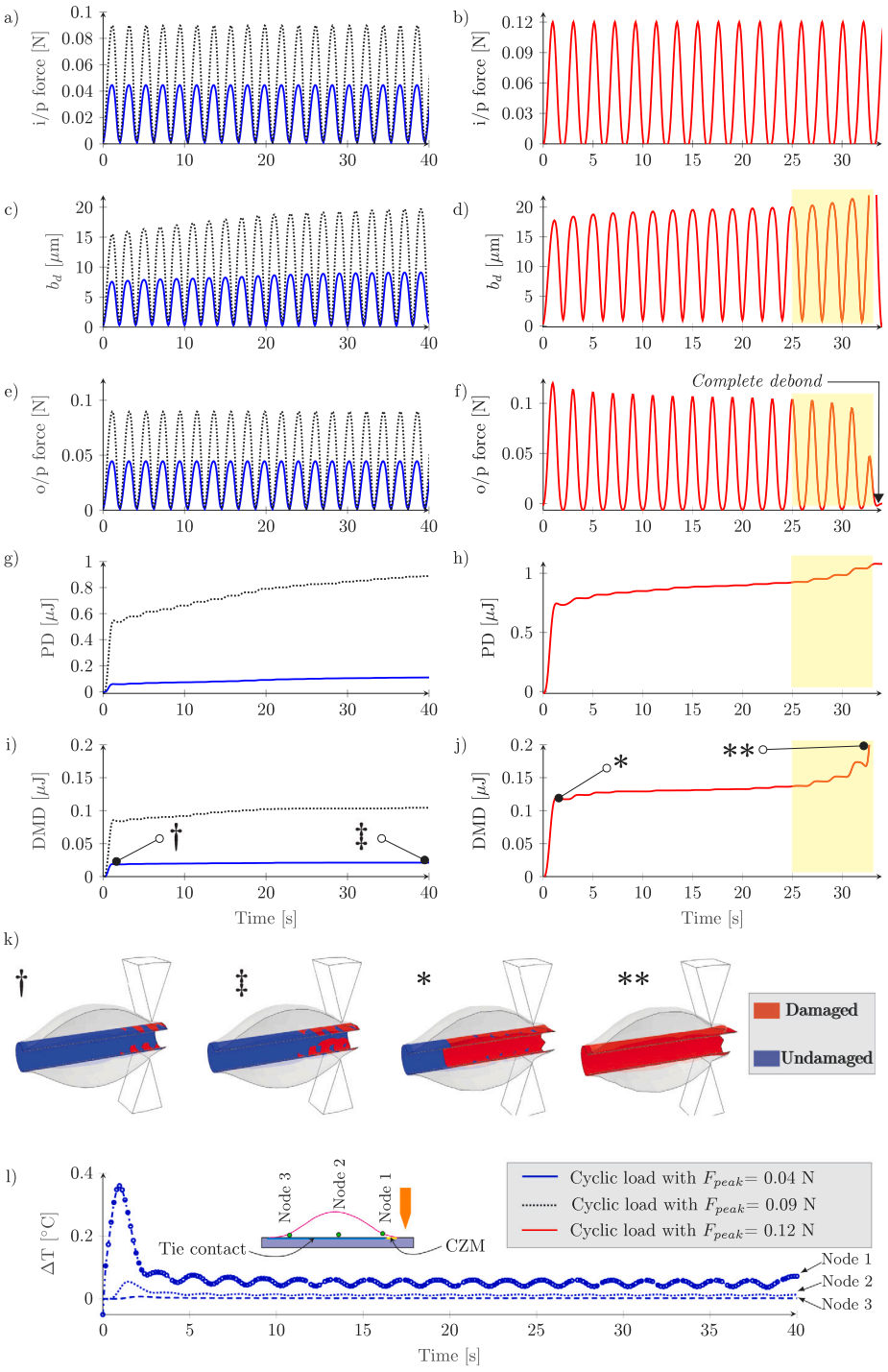

Fig. 9. (a–b) Input force as a function of time; (c–j) output quantities of FE simulations at different loading amplitudes; (k) visualisation of the damaged interface at specific simulation timepoints; (l) nodal temperature distribution for cyclic load with F_{peak} = 0.04 N. The shaded yellow box in (d), (f), (h) and (j) shows the abrupt rise in output quantities closer to the debonding of the droplet.

which steadily increases as the damage propagates at the interface. As the damage propagates, surface area of the damaged region increases, which increases *FD*.

3.4. Reliability and limitations

While promising, microcomposite fatigue testing is currently poorly established. Therefore a discussion on the possible problems and limitations is necessary. One point of consideration is the aforementioned number of fibre loading cycles. Measuring multiple droplets from a single filament greatly reduces effort required in the sample preparation and experiment setup. The scatter in the results of droplets measured from the same filament is also significantly lower as previously reported for quasi-static tests. Further work is required to ensure the repeated loading of the fibre through several droplets does not significantly affect the results due to cumulative effects. Additionally, the free fibre-length changes based on the position of the droplet along the fibre (see Fig. 1). This directly affects the displacement amplitude necessary to reach a certain force level due to the fibre elastic deformation. Thus, in

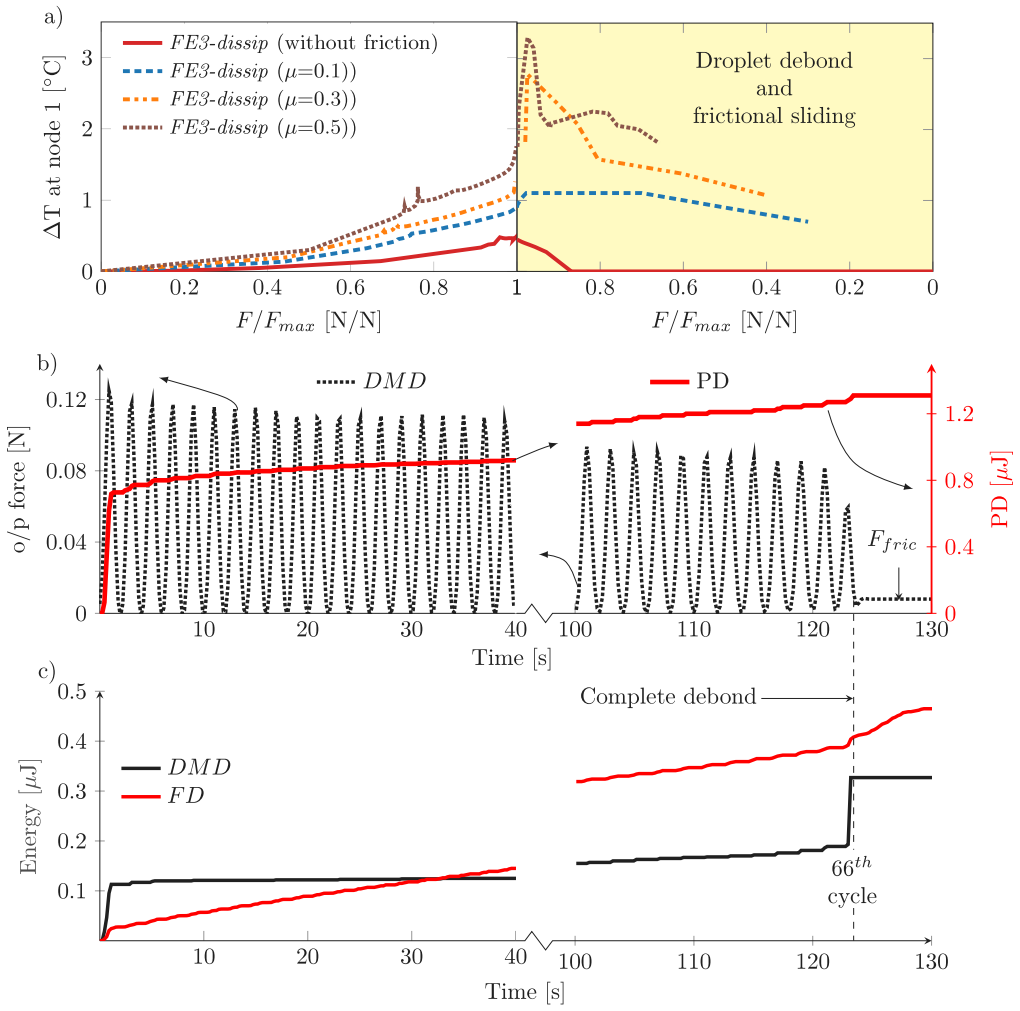

Fig. 10. (a) Simulation results showing the variation of temperature in quasi-static MB test for different values of frictional coefficient's; (b) and (c) different energy quantities extracted from the FE simulations for a cyclic test with interfacial friction with $\mu = 0.1$ used as a coefficient.

addition to the droplet size, the droplet position also contributes to the variation of the test frequency (blade movement speed kept constant). To minimise these factors in this study, the fatigue tests were performed only on droplets from the first 5–8 mm of the whole available 13–14 mm length of the fibre. The rest of the droplets were utilised for quasi-static testing when possible, as the effect of fibre's elastic deformation is mostly negligible in maximum load based analysis of the quasi-static results [14].

A problem also arises from the correlation between droplet size and the performance of the droplet in the test. While most of the samples did not exhibit such correlation, a notable portion did. The phenomenon is most likely related to the droplet degree of cure, which is a known source of uncertainty in microdroplet testing with thermoset resins [10–12]. It is, however, far more pronounced in fatigue testing and the underlying causes need to be identified and addressed before the method can be reliably utilised as more than a qualitative measure. In this study, the issue was mitigated by measuring similar size ranges droplets for both of the two fibre types and identifying the problematic data through analysis. Comparison to other methods and length scales is, however, not reliable until the issue of unpredictable microdroplet curing can be addressed.

Analysis of microcomposite interfacial tests commonly features considerations for two major contributing factors to the measured maximum load: friction and thermal stresses [14,21]. For the micro-fatigue test, while the presence of these factors cannot be argued, no in-depth analysis to their role is included based on the experimental results. The FEA includes the thermal stresses from curing as a part of the model and the role of friction is likewise explored through FEA. It is worth of note that some qualitative correlation between the difference in damage evolution of the two sample types and the difference in frictionless and friction-included FEA: one exhibits sudden and catastrophic damage propagation, and the other a stable propagation and ultimately better fatigue tolerance. Possible explanations include the plasticising effect of the sizing, surface roughness and increased adhesive and/or sliding friction. The analysis of frictional contributions in the micro-fatigue test presents an interesting topic for future work.

Despite the aforementioned challenges, the method can provide valuable additional information about the interphase when coupled with quasi-static methods. At this stage of development, the method already offers unprecedented throughput and robustness (as a testing method) for a fatigue test at this scale. Based on the FE modelling used in characterising the method, the device and samples result in reasonably well-behaving measurements and the test exhibits good sensitivity to different interphase types. With future developments and understanding, the method could potentially provide quantitative data on the fatigue performance of the interphase.

4. Conclusions

In this study, the concept of a micro-fatigue test, based on the well-known microbond test setup was explored. The test exhibited excellent sensitivity to changes at the interphase as represented by two

fibre samples that were identical except for their surface treatments — a clean glass surface and a model sizing comprising an aminosilane coupling agent and an epoxy film former. A clear difference was noted in the fatigue performance at all tested loading levels and a difference in damage propagation was observed both experimentally and in FEA. This represents an important result towards understanding the role of sizing in composites and highlights the need to consider more than maximising the interfacial strength. The presented micro-fatigue test provides a potential methodology for further studies on the topic.

Finite element analysis was used extensively to study various aspects of the micro-fatigue test to identify the advantages and disadvantages of the methodology. The higher strain-rate – used to minimise the time requirement of a single measurement – had a clear but predictable minor effect on the force required to debond the droplets. This was supported by both FEA and experimental observations. Plastic deformation at the meniscus region is a known disadvantage of the microbond test but caused no additional changes in the sample behaviour and the resulting decrease in load level could be compensated in the cyclic testing. Damage evolution during the fatigue test can be qualitatively monitored via these compensations and the results agree well with the trend seen in finite element analysis. FEA analysis of the role of friction shows it can stabilise the damage propagation significantly, which also has possible implications on the mechanism of improvement by the sizing. Overall, the micro-fatigue test presented here is promising novel addition to the increasing selection of microcomposite testing approaches.

CRediT authorship contribution statement

P. Laurikainen: Conceptualization, Methodology, Formal analysis, Investigation, Data curation, Writing – original draft, Writing – review & editing, Visualization. **R. Dsouza:** Conceptualization, Formal analysis, Investigation, Data curation, Validation, Writing – original draft, Writing – review & editing, Visualization. **M. Kakkonen:** Methodology, Software, Resources, Writing – review & editing. **M. Kanerva:** Validation, Resources, Writing – review & editing, Supervision. **E. Sarlin:** Conceptualization, Resources, Writing – review & editing, Supervision.

Declaration of competing interest

The authors declare that they have no known competing financial interests or personal relationships that could have appeared to influence the work reported in this paper.

Data availability

Data will be made available on request.

Acknowledgements

The study was partly financially supported by the Tampere University Graduate School, Finland, Jenny and Antti Wihuri foundation, Finland (Grant No. 00210182), as well as the FibData project: Revolution in Data-based Fibre Material Science using Microrobotics and Computational Modelling funded by the Finnish Foundation for Technology Promotion and the Jane and Aatos Erkko Foundation, Finland and the Academy of Finland postdoctoral project: From micro-scale data to macro-scale understanding for improved safety of composite materials - MicMac (Grant No. 314983). The authors would also like to acknowledge Jesse Savolainen for his help with the LFA measurements.

Appendix A. Supplementary data

Supplementary material related to this article can be found online at https://doi.org/10.1016/j.compositesa.2023.107425.

References

[1] Thomason J. The interface region in glass fibre-reinforced epoxy resin composites: 3. Characterization of fibre surface coatings and the interphase. Composites 1995;26(7):487–98. http://dx.doi.org/10.1016/0010-4361(95)96806-H.
[2] Miller B, Muri P, Rebenfeld L. A microbond method for determination of the shear strength of a fiber/resin interface. Compos Sci Technol 1987;28(1):17–32. http://dx.doi.org/10.1016/0266-3538(87)90059-5.
[3] Fazlali B, Lomov SV, Swolfs Y. Fiber break model for tension-tension fatigue of unidirectional composites. Composites B 2021;220:108970. http://dx.doi.org/10.1016/j.compositesb.2021.108970.
[4] Mai K, Mäder E, Mühle M. Interphase characterization in composites with new non-destructive methods. Composites A 1998;29(9):1111–9. http://dx.doi.org/10.1016/S1359-835X(98)00092-X.
[5] Mäder E, Gao S-L, Plonka R. Static and dynamic properties of single and multi-fiber/epoxy composites modified by sizings. Compos Sci Technol 2007;67(6):1105–15. http://dx.doi.org/10.1016/j.compscitech.2006.05.020.
[6] Brodowsky HM, Jenschke W, Mäder E. Characterization of interphase properties: Microfatigue of single fibre model composites. Composites A 2010;41(11):1579–86. http://dx.doi.org/10.1016/j.compositesa.2010.07.006.
[7] Shin P-S, Kim J-H, Baek Y-M, Park H-S, Park J-M. Epoxy matrix with adding dopamine for improving mechanical property and interfacial adhesion with glass fiber. Compos Res 2019;32(2):96–101.
[8] Schutte CL. Environmental durability of glass-fiber composites. Mater Sci Eng R 1994;13(7):265–323. http://dx.doi.org/10.1016/0927-796X(94)90002-7.
[9] Ishida H. A review of recent progress in the studies of molecular and microstructure of coupling agents and their functions in composites, coatings and adhesive joints. Polym Compos 1984;5(2):101–23. http://dx.doi.org/10.1002/pc.750050202.
[10] Zinck P, Wagner H, Salmon L, Gerard J. Are microcomposites realistic models of the fibre/matrix interface? II. Physico-chemical approach. Polymer 2001;42(15):6641–50. http://dx.doi.org/10.1016/S0032-3861(00)00871-5.
[11] Laurikainen P, Pötz S, Jokinen J, von Essen M, Lindgren M, Kallio P, Kanerva M, Oreski G, Sarlin E. High-throughput mechanical micro-scale characterization of composites and the utilization of the results in finite element analysis. In: Proceedings of the 18th European conference on composite materials. European Society of Composite Materials; 2018.
[12] Bryce D, Thomason J, Yang L. Micromechanical and spectroscopic characterisation of the curing performance of epoxy resins in the microbond test. IOP Conf Ser: Mater Sci Eng 2020;942(1):012019. http://dx.doi.org/10.1088/1757-899x/942/1/012019.
[13] Dsouza R, Antunes P, Kakkonen M, Tanhuanpää O, Laurikainen P, Javanshour F, Kallio P, Kanerva M. Microscale sensor solution for data collection from fibre-matrix interfaces. Sci Rep 2021;11:8346. http://dx.doi.org/10.1038/s41598-021-87723-9.
[14] Laurikainen P, Kakkonen M, von Essen M, Tanhuanpää O, Kallio P, Sarlin E. Identification and compensation of error sources in the microbond test utilising a reliable high-throughput device. Composites A 2020;137:105988. http://dx.doi.org/10.1016/j.compositesa.2020.105988.
[15] Dsouza R, Antunes P, Kakkonen M, Jokinen J, Sarlin E, Kallio P, Kanerva M. 3D interfacial debonding during microbond testing: Advantages of local strain recording. Compos Sci Technol 2020;195:108163. http://dx.doi.org/10.1016/j.compscitech.2020.108163.
[16] Lin W-Q, Zhang Y-X, Wang H. Thermal conductivity of unidirectional composites consisting of randomly dispersed glass fibers and temperature-dependent polyethylene matrix. Sci Eng Compos Mater 2019;26(1):412–22.
[17] Nagy B, Nehme SG, Szagri D. Thermal properties and modeling of fiber reinforced concretes. Energy Procedia 2015;78:2742–7.
[18] Boyer R, Welsch G, Collings E. 32. Ti-6Al-4V. In: Materials properties handbook - titanium alloys. ASM International; 1994, p. 513–6.
[19] Harvey PD. 4.8 AISI Type 304. In: Engineering properties of steel. ASM International; 1982, p. 273–80.
[20] Lee Y-L, Pan J, Hathaway RB, Barkey ME. 4.2 The stress-life (S-N) and fatigue limit testing. In: Fatigue testing and analysis - theory and practice. Elsevier; 2005.
[21] Zhandarov S, Mäder E. Peak force as function of the embedded length in pull-out and microbond tests: effect of specimen geometry. J Adhes Sci Technol 2005;19(10):817–55. http://dx.doi.org/10.1163/1568561054929937.